Electronic Supplementary Information

Is the catalytic current always proportional to the surface of electro-catalyst?

Emily Dominique[a], Christophe Renault [a*]

[a]Department of Chemistry & Biochemistry, Loyola University Chicago, Flanner Hall, 1068 W Sheridan Road, Chicago, Illinois 60660, USA

Email: crenault@luc.edu

Table of Contents

1. Numerical Modeling

General definition. A finite-element simulation software, COMSOL Multiphysics v6.3, was used to solve for the diffusion of a redox species N_2H_4 toward an electrode with a fractional surface coverage of nanoparticles. Under sole diffusion, the concentration of the N_2H_4 species, C_{N2H4}, is governed by 2nd Fick's law:

$$\frac{\partial C_{N_2H_4}}{\partial t} = D\Delta C_{N_2H_4} \qquad \text{Eq. S1}$$

where t, D and Δ are the time, diffusion coefficient of hydrazine and Laplacian operator, respectively. The complex mechanism of hydrazine oxidation is reproduced with a phenomenological model comprising two steps: (i) a slow and irreversible two-electron oxidation reaction leading to an intermediate "A" followed by (ii) a fast two-electron transfer. The overall number of electron exchange is $n_{tot} = 4$ but the rate determining step involves only $n_{rds} = 2$ electrons.

$$N_2H_4 \xrightarrow{k_{\text{rds}}} A + 2e^- \xrightarrow{k_{\text{fast}}} N_2 + 4H^+ + 2e^-$$

The kinetics of the first two-electron transfer is described by a standard rate of electron transfer, k_{rds}, in the Butler-Volmer formalism.

Geometry. For the simulation of a homogeneous electrode (i.e. bare gold) shown in the main text in **Figure 2C**, a 1D domain (segment) was used. For the simulation of a network of nanoparticle we used the approach from Amatore et al. A 2D hexagonal arrangement of nanoparticles is approximated by a 2D axial cell reducing a 3D problem into a simpler 2D problem.[1] The 2D axial geometry is shown in **Figure S1A** along with the boundaries of the domain of simulation. Adjacent to the axis of symmetry (z) lays the "nanoparticle" of radius r_{NP}. This later is represented with a hemisphere to reduce computational burden while recreating the 3D character of the nanoparticle. The total radius of the simulation cell, r_{cell}, is defined using the relation:

$$r_{cell} = r_{NP}\sqrt{\frac{2-\theta}{\theta}} \qquad \text{Eq. S2}$$

where $\theta = S_{NP}/S_{total}$ is the fraction of nanoparticle's surface over the entire surface. The surface of the nanoparticle is defined as $S_{NP} = 2\pi {r_{NP}}^2$ (i.e. hemisphere's surface) and the entire projected surface is defined as $S_{total} = \pi(r_{NP}^2 + r_{cell}^2)$. The geometry is automatically adjusted when the value of θ is changed. The height of the domain of simulation, H, is defined by the relation

$$H = 6\sqrt{D \times t_{tot}} \qquad \text{Eq. S3}$$

where t_{tot} is the total time of the experiment. This relation ensures the diffusion layer does not reach the boundary representing the bulk of the solution (boundary 1 in **Figure S1A**). Hence, a semi-infinite condition is emulated.[2] For cyclic voltammetry the value of t_{tot} is defined as $2|E_{max} - E_{min}|/v$ where E_{max}, E_{min} and v are the maximum and minimum of the potential window as well as the scan rate, respectively.

Mesh. A typical mesh is shown in **Figure S1B**. Finer elements are used near the electrode and especially their edges to accurately capture the steep gradient of concentration. A distributed element-size is used to correctly capture the concentration gradient further away from the surface while reducing the number of elements. A typical range of elements in our simulation is 3,000-10,000. For cyclic voltammetry (CV) the time of computation is typically 0.5 - 1 min

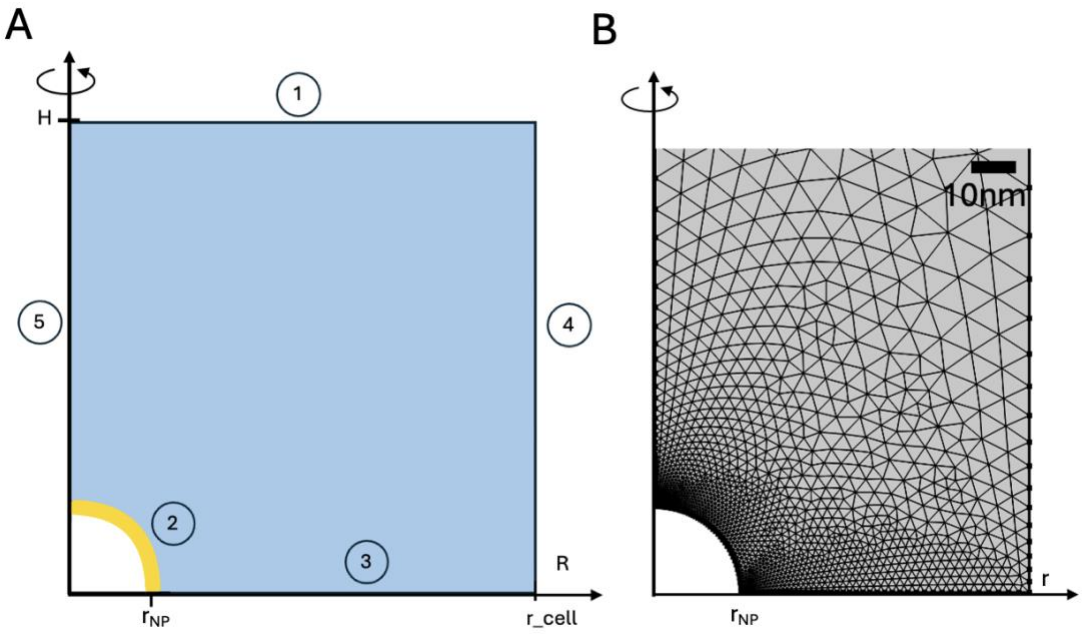

Figure S1. Schematic of the 2D axial geometry used to represent the solution (blue color), the nanoparticle (boundary 2) and HOPG (boundary 3). The axis of revolution (boundary 5) and the right boundary of the cell (boundary 4) are set as mirror boundaries to emulate an array of nanoparticles. (B) Example of mesh. The size and shape of the mesh is adapted to follow the gradients of concentration near the nanoparticle.

Boundaries. A Neumann boundary condition, set by the Butler-Volmer equation,[2] was used on the boundaries 2 and 3 to represent the kinetics of electron transfer at the nanoparticle and substrate, respectively. For simulation of cyclic voltammograms, the current flux is given by:

$$j = n_{tot} k_{rds} F C_{N_2H_4} \left[e^{(1-\alpha) n_{rds} \frac{F}{RT} (E_{WE} - E^{0\prime})} \right] \quad \text{Eq. S4}$$

where F, R, T, E_{WE}, n_{tot}, α, k_{rds}, $n_{rds}$and $E^{0\prime}$ are the Faraday's constant, the ideal gas constant, the temperature, the potential of the working electrode, the total number of electrons transferred, the symmetry coefficient, the standard rate of electron transfer, the number of electrons in the rate determining step and the apparent standard potential of the redox reaction, respectively. The standard rate of electron transfer must be understood as a phenomenological parameter that incorporates multiple elementary steps such as adsorption of hydrazine and thus will depend on the nature of the electrode (i.e. gold vs HOPG). The "bulk" of the solution is represented by a Dirichlet boundary condition where the concentration of hydrazine at any time is equal to the initial concentration C^0. Finally, the axis of symmetry and right boundary (**Figure S1**) are described by mirror boundaries ($\nabla C_{N_2H_4} = 0$). All the boundaries are summarized in the **Tables S1** and **S2**.

Table S1. Boundary conditions for the simulation of CV.

#	Definition	Boundary
1	Bulk solution	$C_{N_2H_4} = C^0$
2	Nanoparticle surface	$j = n_{total} k_{rds} F C_{N_2H_4} \left[e^{\left[\frac{(1-\alpha) n_{rds} F}{RT}\right](E_{WE} - E^{0\prime})} \right]$
3	HOPG surface	$j = n_{total} k_{rds} F C_{N_2H_4} \left[e^{\left[\frac{(1-\alpha) n_{rds} F}{RT}\right](E_{WE} - E^{0\prime})} \right]$
4	Side boundary	$\frac{\partial C_{N_2H_4}}{\partial r} = 0$

Initial parameters. The initial parameters are provided in **Table S2**. A range of parameter is given when the parameter was adjusted.

Table S2. List of parameters used in the numerical models of CV

Name	Expression	Description
Physical constants		
F	96485 C.mol^{-1}	Faraday's constant
R	8.314 J.K^{-1}.mol^{-1}	ideal gas constant
T	298 K	temperature
Redox couple		
C^0	1 mM	Initial concentration of N_2H_4
$E^{0\prime}$	-0.100 V	Apparent standard potential
k_{rds}	Gold: 3x10^{-9} m.s^{-1} HOPG: 1x10^{-20} m.s^{-1}	Electron transfer standard rate constant[a]
α	0.5	symmetry coefficient

n_{tot}	4	Total number of electrons transferred
n_{rds}	2	number of electrons transferred in rate determining step
D	7.1 x10^{-6} cm^2.s^{-1}	diffusion coefficient
SAM & pinhole		
r_{NP}	25 nm	Radius of nanoparticle
A	0.0314 cm^2	experimental surface of the working electrode
θ	1.0 - 6 x10^{-6}	Nanoparticle coverage
Cell		
r_{cell}	$r_{cell} = r_{NP}\sqrt{\frac{2-\theta}{\theta}}$	width of cell
H	$6\sqrt{D \times t_{tot}}$	height of cell
Electrochemical measurement		
v	0.05 V/s	scan rate
E_{min}	-0.1 V	initial and final potential of CV
E_{max}	0.6 V	vertex potential of CV
t_{tot}	$2\lvert E_{max} - E_{min}\rvert / v$	total time of CV

[a]**Note**: k_{rds} depends on the nature of the electrode (ie HOPG vs gold).

Final quantities. The currents over the nanoparticle (i_{NP}) and the HOPG (i_{HOPG}) are obtained by integration of the flux over the relevant boundaries:

$$i_{NP} = 2\pi \int_0^{r_{NP}} j(r)dr \qquad \text{Eq. S5}$$

$$i_{HOPG} = 2\pi \int_{r_{NP}}^{r_{cell}} j(r)dr \qquad \text{Eq. S6}$$

where $j(r)$ is the current density computed along the boundary at the position r. The factor 2π comes from the integration over the axis of symmetry. The current densities of an array are calculated by dividing the currents by the total surface of the cell, πr_{cell}^2. Finally, the total current density, j, is obtained by adding the two contributions $j = j_{\mathrm{NP}} + j_{\mathrm{HOPG}}$.

2. Experimental Section

Reagents. Hydrazine (98%), ferrocenemethanol (97%) noted FcMeOH, sulfuric acid (95.0-98.0%), gold (III) chloride trihydrate (> 99.9%), sodium nitrate (> 99.9%), potassium phosphate monobasic (≥ 99.0%), potassium phosphate dibasic (≥ 98.0%), potassium chloride (99.0-100.5%), agarose, potassium nitrate (≥ 99.0%) were purchase from Sigma Aldrich (USA) and used without further purification. Deionized water (18.2 MΩ.cm) was obtained from a Barnstead MicroPure water purification system with a 0.2 µM ultra-filtration membrane. Potassium phosphate buffer at 100 mM was prepared using potassium

phosphate dibasic and monobasic forms. The pH was measured to be 7.0 using a Ohaus pH meter.

Electrochemical Measurements. A CH601E potentiostat from CH Instruments (Austin, TX) and a home-made Faraday cage were used. The working, counter and reference electrodes were a 20 mm X 20 mm diameter HOPG grade AB sheet purchased from SPI supplies (West Chester, PA), 0.5 mm diameter x 32 mm long platinum wire (purchase from CH Instruments, Austin, TX) and a Ag/AgCl 1 M KCl from CH Instruments (Austin, TX), respectively. The reference electrode was placed in a salt bridge to avoid contamination of the reference by hydrazine. The salt bridges were prepared by filling a glass Pasteur pipette with molten agarose gel (3%$_m$ in 1 M KNO_3 aqueous solution) and letting the gel cool down inside the pipette. Bridges were stored in large volumes of 1 M KNO_3 and changed regularly to avoid cross-contamination. Note all measurements were taken in 0.1 M phosphate buffer pH 7.0 with 0.4 M KNO_3 to avoid ohmic drop. The cell was not disassembled between electrodeposition of the nanoparticles, voltammetry of ferrocenemethanol and hydrazine oxidation to ensure a constant surface. The surface of the HOPG exposed to solution was delimited by a 8.5 mm diameter O-ring made of Viton pressed onto the HOPG with a home-made Teflon cell. Prior to the electrodeposition of the array the HOPG sheet was cleaved with clear scotch tape.

Electrodeposition and Characterization of Gold Nanoparticles on HOPG. Gold nanoparticles were deposited using constant potential electrolysis. The HOPG was submerged in 0.1 M $NaNO_3$ solution containing 0.25 mM $3(H_20)HAuCl_4$. The electrolysis potential was always 0.7 V, while the duration was varied from 1 second to 1,200 seconds. The option “disconnect cell between runs” was selected in the CH Instrument software to ensure that no deposition occurs when the instrument is not recording.

3. Determination of θ by SEM and electrochemical

A Hitachi SU3500 model was used with an accelerating voltage of 30 kV and a working distance between 6.0 mm and 6.4 mm. The array of gold nanoparticles was rinsed with DI H2O and dried in an oven at 100°C before imaging. ImageJ software was used to determine the fraction of nanoparticles on the surface. **Figure S2** shows a typical SEM image for various electrodeposition times (A) 1200 s (B) 900 s (C) 90 s (D) 1 s of gold nanoparticles onto HOPG substrate.

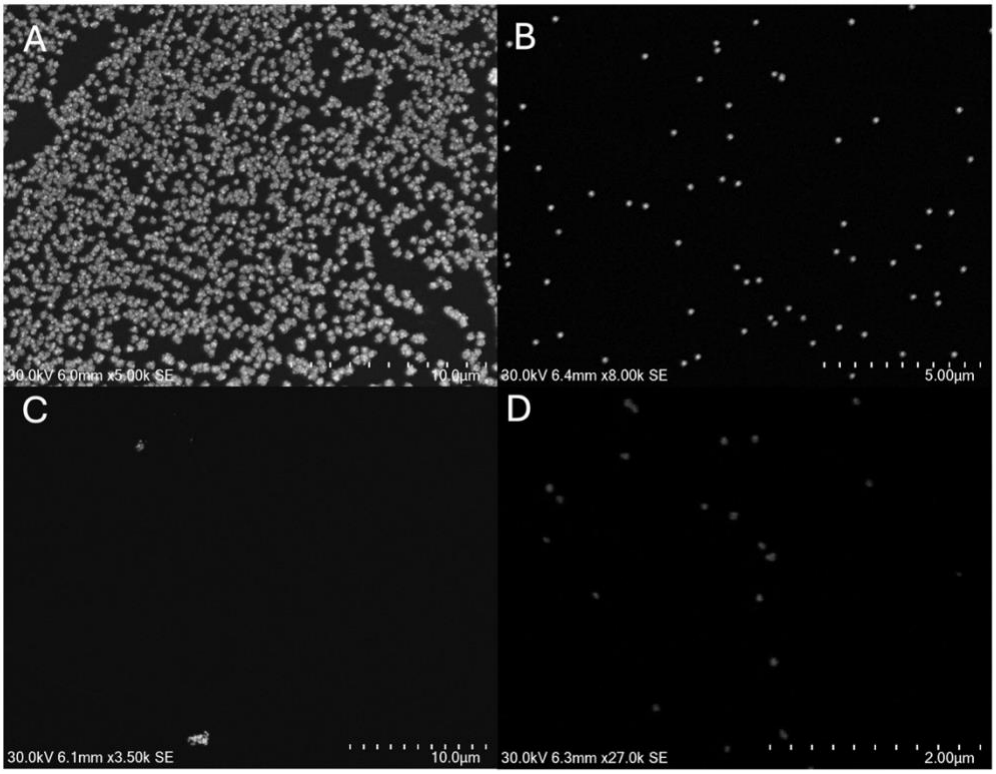

Figure S2. A typical SEM image for various electrodeposition times A) 1200 s B) 900 s C) 90 s D) 1 s at 0.7 V of gold nanoparticles onto HOPG substrate.

The surface of gold was also characterized by continuously cycling the electrode's potential between 0.2 V and 1.4 V at 100 mV/s in 0.1 M H_2SO_4 until no change was observed between scans (typically after 30 cycles). **Figure S3** shows CVs of a modified HOPG substrate with gold nanoparticles deposited for different time lengths (A) 1200 s (B) 900 s (C) 90 s (D) 1 s recorded in 0.1M H_2SO_4. Each modified substrate is cycled 30 times and only the last complete CV is plotted. The area under the gold reduction peak is measured after 30 cycles. The surface area of the gold nanoparticles was determined by integration of the gold reduction peak and using an average charge for a reduction of a gold oxide monolayer of 410 $\mu C.cm^{-2}$ [1,4-9].

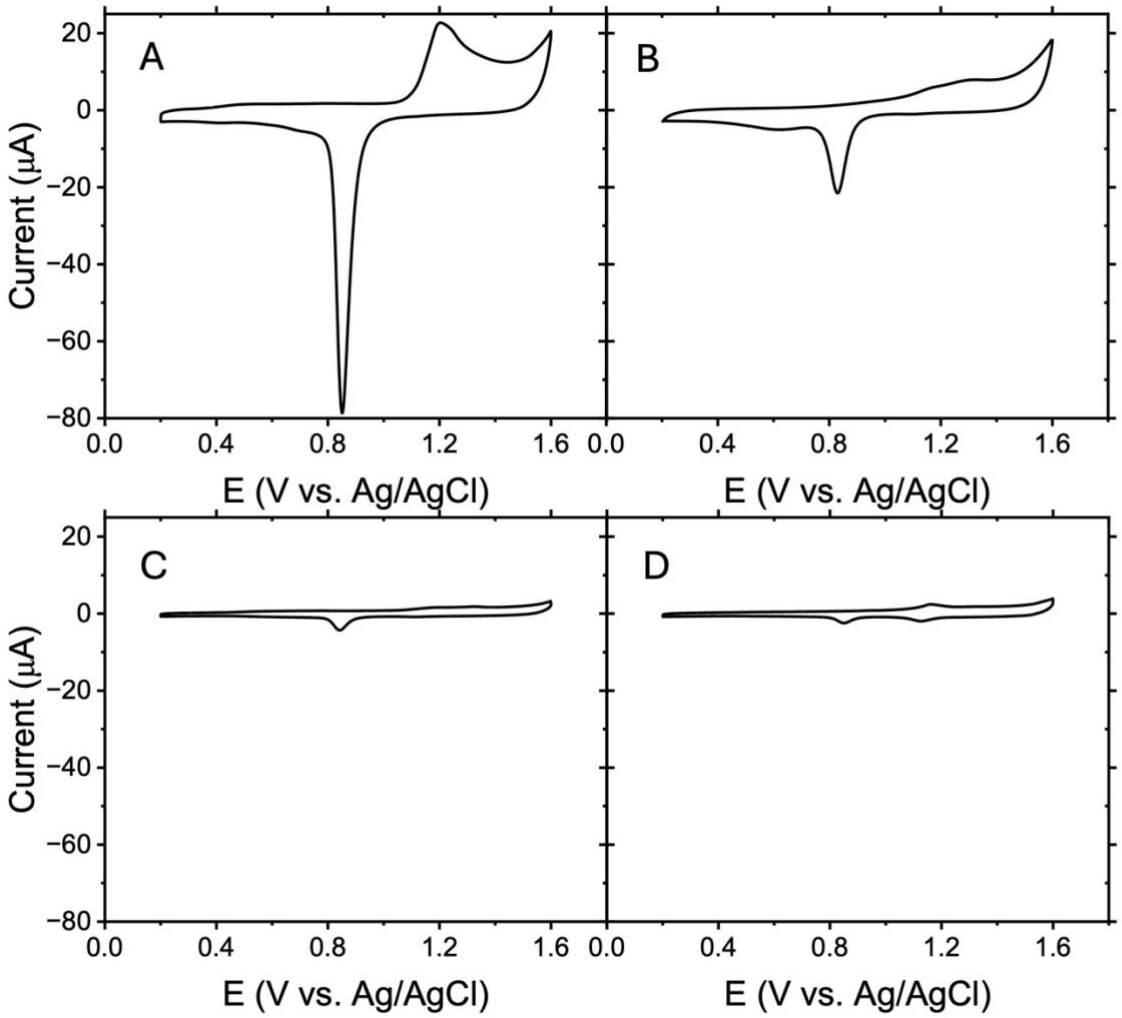

Figure S3. CVs obtained with an HOPG substrate modified with various amounts gold nanoparticles determined by electrodeposition time A) 1200 s B) 900 s C) 90 s D) 1 s successfully immersed in an aqueous solution containing 0.1 M H_2SO_4. The scan rate is v = 0.1 V/s.

4. Determination of the Geometric Surface via voltammetry of Ferrocene Methanol

Just after experiments on hydrazine the cell was rinsed vigorously with water, then filled with of 1 mM FcMeOH in in 0.1 M phosphate buffer pH 7.0 and 0.4 M KNO_3. Then, a CV was acquired at v = 0.05 V/s. **Figure S4** shows a typical experimental CV. The anodic peak height, i_p, is measured after correction from capacitive current. Finally, the Randles-Sevcik equation below was used to extract the geometric surface area A.[3]

$$i_p = (2.69\ x\ 10^5) n^{\frac{3}{2}} A D_O^{\frac{1}{2}} C_{FcMeOH} v^{\frac{1}{2}} \qquad \text{Eq. S7}$$

Using an O-ring of 8.5 mm diameter ($\pi \times 0.425 \times 0.425 = 0.567\ \text{cm}^2$), the geometric surface area was calculated to be 0.608 $\pm$ .059 cm^2. For a gold electrode with a diameter of 2 mm the surface area was calculated to be 0.0292 cm^2.

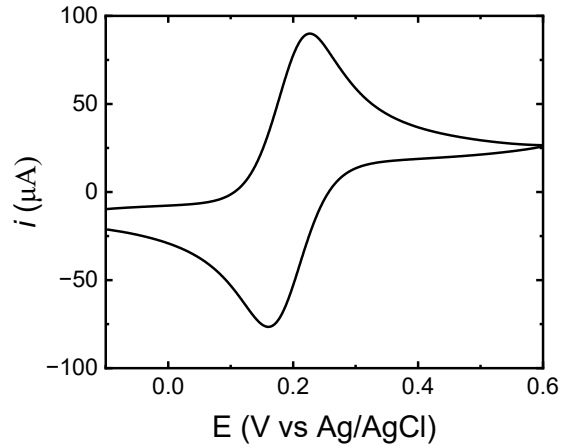

Figure S4. Cyclic voltammograms obtained with an HOPG substrate modified with gold nanoparticles and immersed in an aqueous solution containing 1.00 mM of FcMeOH and 0.1 M phosphate buffer (pH 7.0). The scan rate is v = 50 mV/s.

5. Determination of k_{rds} of Bare Gold Electrode

Figure S5 shows the experimental CVs recorded in 1 mM hydrazine 0.4 M KNO_3, 0.1 M phosphate buffer pH 7.0 with a 2 mm diam. bare gold electrode. Between each measurement the gold electrode was cycled 30 times in 0.1 M H_2SO_4 as described in **Figure S3**. Variability in voltammetry is observed when the number of cycles in 0.1 M H_2SO_4 changes. **Figure S5** also shows CVs simulated for a bare gold electrode only adjusting for different values of k_{rds}. The value of α is kept at 0.5 for all CVs. The orange, red, purple, pink, blue, cyan, black and green traces correspond to k_{rds} values of 2.0 x10^{-9} m.s^{-1}, 6.5 x10^{-9} m.s^{-1}, 2.3 x10^{-9} m.s^{-1}, 8.0 x10^{-9} m.s^{-1}, 4.0 x10^{-9} m.s^{-1}, 7.3 x10^{-9} m.s^{-1}, 3.3 x10^{-9} m.s^{-1}, 9.9 x10^{-9} m.s^{-1}

respectively. These values average to 5.4 $\pm$ 2.9 x10^{-9} m.s^{-1}. While oxidizing and reducing the gold nanoparticles in 0.1 M H_2SO_4 different facets of gold are exposed[4]. Alvarez-Ruiz et. al report varying CV response of 1mM N_2H_4 dependent on gold facets, such as Au(100), Au(110), and Au(111) in acidic conditions[5]. As the gold facets that are exposed may vary between experiments an average k_{rds} is used.

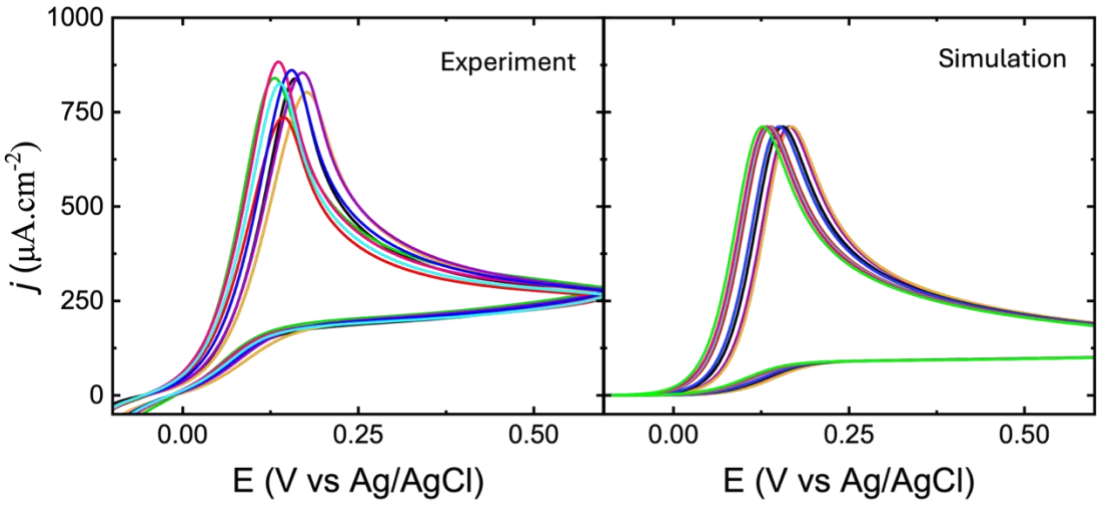

Figure S5. Experimental and simulated CVs of the oxidation of 1 mM N2H4 in 0.4 M KNO3 0.1 M phosphate buffer pH 7.0 on a bare gold electrode. The scan rate is v = 50 mV/s. The currents are normalized by the apparent surface of the gold disk (0.0292 cm^2). The simulated orange, red, purple, pink, blue, cyan, black and green traces correspond to krds values of 2.0 x10^{-9} m.s^{-1}, 6.5 x10^{-9} m.s^{-1}, 2.3 x10^{-9} m.s^{-1}, 8.0 x10^{-9} m.s^{-1}, 4.0 x10^{-9} m.s^{-1}, 7.3 x10^{-9} m.s^{-1}, 3.3 x10^{-9} m.s^{-1}, 9.9 x10^{-9} m.s^{-1} respectively. The experimental parameters are v = 0.05 V/s, α = 0.5, C_{N2H4}= 1 mM, D = 7.1x10^{-6} cm^2.s^{-1}, $E°'$ = -0.100 V vs Ag/AgCl.

6. Concentration profiles of high and low θ

Figure S6 shows concentration profiles obtained during the 2D simulation of CV (slice taken at 0.6 V) of hydrazine oxidation on a gold nanoparticle array with "low" θ = 4x10^{-4} and "high" θ = 0.2. These profiles reveal a spherical concentration gradient at low coverage (tilted arrow) while the gradient becomes normal to the HOPG surface at higher coverage. This illustrates the progressive transition between overlapping and non-overlapping

diffusion layers.

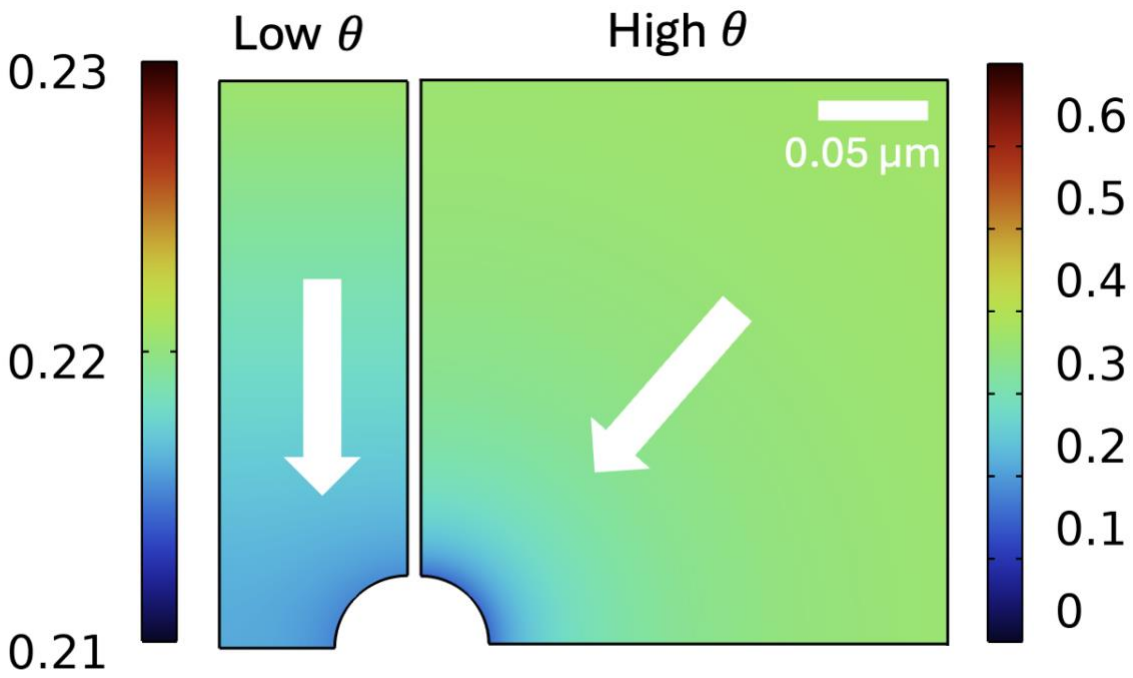

Figure S6. Typical concentration profiles from the simulation of a high and low theta. The parameters of the simulation are v = 0. 05 V/s, [N_2H_4] = 1 mM, "low" θ = 4 x 10^{-4} and "high" θ = 0.2, n_{tot} = 4, n_{rds} = 2, α = 0.5, $E^{0'}$ = 0.100 V, D = 7.1 $cm^2.s^{-1}$and r_{NP} = 25 nm. The kinetics of N_2H_4 oxidation on gold and HOPG are represented with a k_{rds} of 3 x10^{-9} $m.s^{-1}$ and 1 x10^{-20} $m.s^{-1}$, respectively.

7. 1D Simulation for determining k_{app}

Figure S7 shows experimental CVs at various θ values in 1mM N_2H_4, 0.4 M KNO_3, and pH 7.0 0.1 M phosphate buffer. **Figure S7** also shows simulated CVs using a 1D model for a homogeneous electrode where the only adjustable parameter is k_{app} of gold.

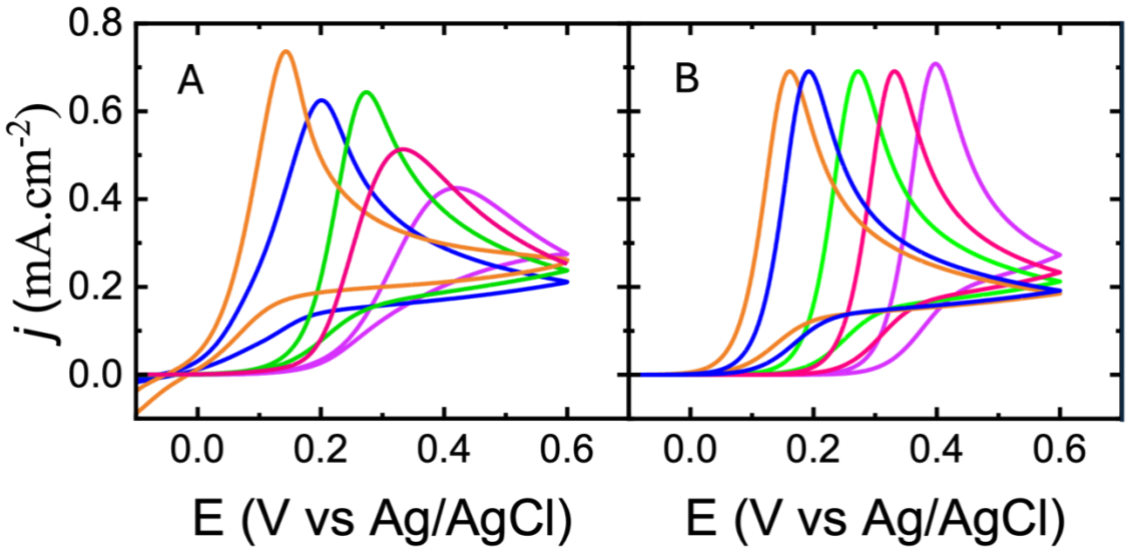

Figure S7. (A) CVs of to N_2H_4 oxidation for various coverage of gold. The trace corresponds to bare gold. The experimental blue, green, pink and violet traces were recorded on a 0.5675 cm^2 HOPG electrode covered with θ_{SEM} = 0.22, 0.1, 0.013 and 0.008, respectively. For all CVs v = 0. 05 /s, [N_2H_4] = 1 mM, [KNO_3] = 0.4 M, [phosphate buffer] = 0.1 M and pH 7.0. (B) Simulated CVs of the oxidation of 1 mM N_2H_4 in 0.4 M KNO_3 0.1M phosphate buffer pH 7.0 on a bare gold electrode. The scan rate is v = 50 mV/s. The currents are normalized by the apparent surface of the gold disk (0.0314 cm^2). A 1D domain (segment) was used. The orange, blue, green, pink, and purple traces correspond to k_{app} of gold 3 x10^{-9} m.s^{-1}, 6 x10^{-10} m.s^{-1}, 4 x10^{-11} m.s^{-1}, 4x10^{-12} m.s^{-1}, 3x10^{-13} m.s^{-1}, respectively. The other parameters are D = 7.1 cm^2.s^{-1}, C_{N2H4} = 1.0 mM, $E°'$ = - 0.10*0* V vs Ag/AgCl.

The regional boundary seen in **Figure 2C** is determined by simulating CVs using a wide range of k_{rds} of gold (1x10^{-7} m.s^{-1} - 1x10^{-14} m.s^{-1}) and θ (1-0.00001) values. Peak height remains constant adjusting k_{rds} while θ is constant. Ideal peak heights (i_{ideal}) were determined by measuring peak height of the simulation when $\theta = 1$ and % change of peak height was measured **Eq. S8.**

$$\%\ Change = \frac{i_{ideal} - i_{peak}}{i_{ideal}} \times 100 \qquad \text{Eq. S8}$$

When % change is over 6% the anodic peak is no longer considered ideal and therefore is no longer within the linear region. Considering the large error bars of θ a transition region is determined between the linear and non-linear region as seen in **Figure 2C** as the orange region. The transition region occurs between $\theta = 0.01$ (6.26% Change) and $\theta = 0.001$ (69.6% Change).

References

1. C. Amatore, J. M. Savéant and D. Tessier, *Journal of Electroanalytical Chemistry and Interfacial Electrochemistry*, 1983, **147**, 39-51.
2. L. R. F. Allen J. Bard, Henry S. White, *Wiley*, 2022.
3. L. F. A. Bard, *Electrochemical Methods: Fundamentals and Applications, 2nd Edition*, Wiley, 2000.
4. A. R. Silva Olaya, B. Zandersons and G. Wittstock, *ChemElectroChem*, 2020, **7**, 3670-3678.
5. B. Álvarez-Ruiz, R. Gómez, J. M. Orts and J. M. Feliu, *Journal of The Electrochemical Society*, 2002, **149**, D35.